Chapter 18

Conodont Apatite: Structure and Geochemistry

Judith Wright

Battelle Pacific Northwest Laboratories, Battelle Boulevard, P.O. Box 999, Richland, WA 99352

Introduction

During the last twenty years our knowledge and understanding of the ultrastructure and geochemical properties of the apatite biominerals of conodont elements has increased dramatically. This is an exciting period in which to be a conodont researcher because we have discovered that the apatite remains of this tiny organism hold the secrets of oceanic, tectonic, and environmental changes locked within the calcium phosphate crystal lattice. The record of synchronous paleochemical events thus retained in conodont apatite provides the quantitative basis for trace element chemostratigraphic correlations as well as paleoceanic and paleogeographic reconstructions.

The soft-bodied impression of the conodont animal (Plate 1) was discovered recently (Briggs, Clarkson and Aldridge, 1983) on a bedding plane of the Lower Carboniferous Granton shrimp bed in Scotland. The first organism found is 40.5 mm in length, 1.8 mm across, and has ray-supported caudal and posterior fins strongly suggesting a nektonic mode of existence. The only hard parts are the conodont elements, or "teeth", which are preserved in the mouth region of the animal. The exact function of these groups of elements, collectively referred to as an apparatus in a single individual, has not been resolved. The main hypotheses are that the apparatus was either a grasping and shredding device involved in the feeding process or a support mechanism for ciliated tentacles used as a food-gathering or respiratory organ. This specimen and subsequent discoveries of other conodont specimens of the same animal with soft tissue preserved (Mikulic *et al.*, 1985a,b; Aldridge *et al.*, 1986; Aldridge *et al.*, 1988) have ended the more than one hundred year old debate on the nature of the conodont animal and have provided an abundance of information for future debates on the affinities of the organisms and the function of their apatitic elements and apparatuses.

Conodont elements were discovered and described by Pander (1856), who considered them to be the teeth of an extinct group of fish. He thought they were composed of calcium carbonate with some associated calcium phosphate. Harley (1861) found that conodont elements were composed of calcium phosphate. Ellison (1944) demonstrated quantitatively that conodont elements are composed of calcium phosphate with the crystal structure of apatite, and Hass and

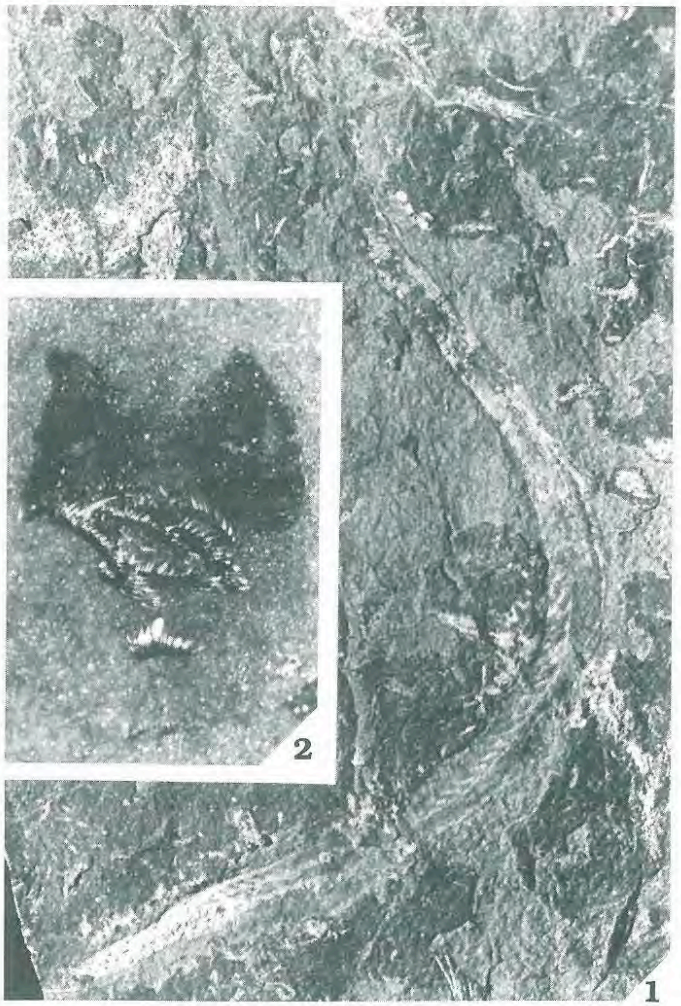

Plate 1. *Clydagnathus* ? cf. *cavusformis* Rhodes, Austin & Druce. Fig. 1. The conodont animal (the head at the top), specimen no. 13821, British Geological Survey, Edinburgh, x 7. Fig. 2. Conodont elements on the counterpart of the head region, under toluene immersion, specimen no. 13822, British Geological Survey, Edinburgh, x 25. Photographs by K.J. Ingham. Courtesy of R.J. Aldridge, 1989.

Skeletal Biomineralization: Patterns, Processes and Evolutionary Trends. Volume I. Joseph G. Carter, editor. Van Nostrand Reinhold, New York.

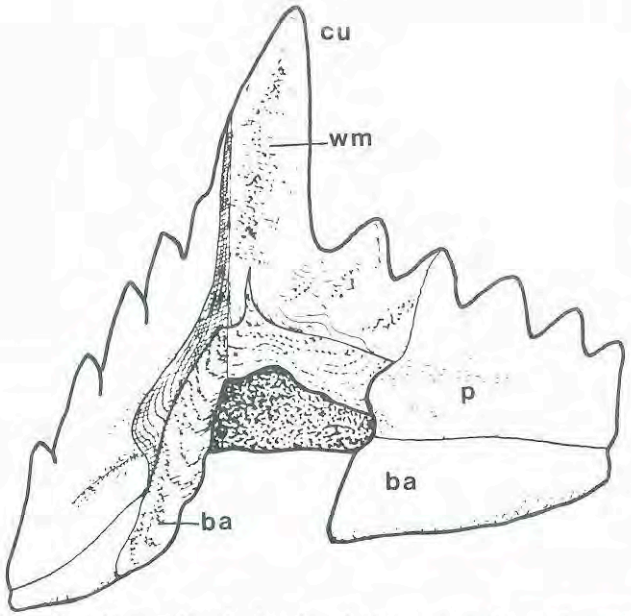

Fig. 1. Generalized simple platform conodont element showing main parts and their orientations: ba = basal body or filling; the crown is composed of: cu = cusp or denticle, p = platform, wm = white matter. From Lindström (1973) by permission of the Geological Society of America.

Lindberg (1946) demonstrated that the individual crystallites are optically continuous. Pietzner *et al.* (1968) determined a general non-stoichiometric formula for conodont apatite:

$$Ca_5Na_{0.14}(PO_4)_{3.01}(CO_3)_{0.16}F_{0.73}(H_2O)_{0.85}$$

Several studies have shown that in addition to the major substituents more than 40 trace element cationic species substitute for calcium (Pietzner *et al.*, 1968; Bradshaw *et al.*, 1972; Wright, 1985; Wright *et al.*, 1987a,b). Furthermore, isotopic ratios of uranium, strontium, neodymium, samarium, and possibly oxygen, represent the isotopic abundances of seawater at the site and time of deposition (Kovach and Zartman, 1981; Kovach, 1980; Burke *et al.*, 1982; Shaw, 1985; Keto, 1987; Luz *et al.*, 1983; Geitgey and Carr, 1987). Isotopic studies make it possible to assign absolute ages to conodont-bearing rocks, trace weathering rates, model oceanic versus continental crustal evolution, ascertain connections between marine water masses, and determine relative paleotemperature fluctuations.

Some Observations on Crystal Chemistry

Conodont elements are generally 0.1 to 3.0 mm in length, although platform elements of Late Devonian *Palmatolepis perlobata* have been reported as long as 12 mm (Sandberg and Ziegler, 1979), and ramiform elements of Late Ordovician *Promissum pulchrum* were reported up to 14 mm long (Aldridge *et al.*, 1988). Conodont elements grew by concentric accretion of apatite lamellae around a central basal cavity or pit (Figure 1). The lamellae are 0.2 to 0.5 μm thick and are composed of approximately parallel crystallites, which are in turn composed of microcrystallites arranged with prism surfaces parallel to the direction of growth (see Figure 2 and Barnes, Sass, and Poplawski, 1973; Lindström and Ziegler, 1981; Szaniawski, 1987; Wright and Conca, 1988).

Apatite belongs to the hexagonal system, in the space group $P6_3/m$. It is characterized by a six-fold c-axis that is perpendicular to three a-axes arranged at 120° angles to one another. The basic formula for the smallest structural component, the unit cell, is: $Ca_{10}(PO_4)_6(OH,F,Cl)_2$ (Deer, *et al.*, 1975). F^- and Cl^- substitute partially or completely for $(OH)^-$, producing changes in lattice parameters because of differences in ionic radii of the substituents. These structural changes give the following comparative stability of apatite compounds: F-Ap>OH-Ap>Cl-Ap (LeGeros, 1981). Carbonate is a principal substituent in low-temperature biogenic apatite, substituting primarily for $(PO_4)^{3-}$ and also for $(OH)^-$. Substitution of $(CO_3)^{2-}$ for $(PO_4)^{3-}$ causes expansion in the c-axis and contraction in the a-axis dimensions, whereas $(CO_3)^{2-}$ for $(OH)^-$ substitution produces the opposite sense of distortion to the crystal structure (LeGeros, 1981). Increasing carbonate substitution decreases apatite stability (LeGeros, 1981; Jahnke, 1984).

A comparison of lattice parameters of biogenic, sedimentary, and igneous apatites is given in Table 1. Conodont apatite generally has an a-axis dimension close to that of marine phosphorites and smaller than that of human teeth and bones. However, the c-axis dimension of conodont apatite is larger than other apatites except SrF-igneous apatite. Distortion in the c-axis indicates that $(CO_3)^{2-}$ substitution in conodonts is predominantly in the $(PO_4)^{3-}$ position.

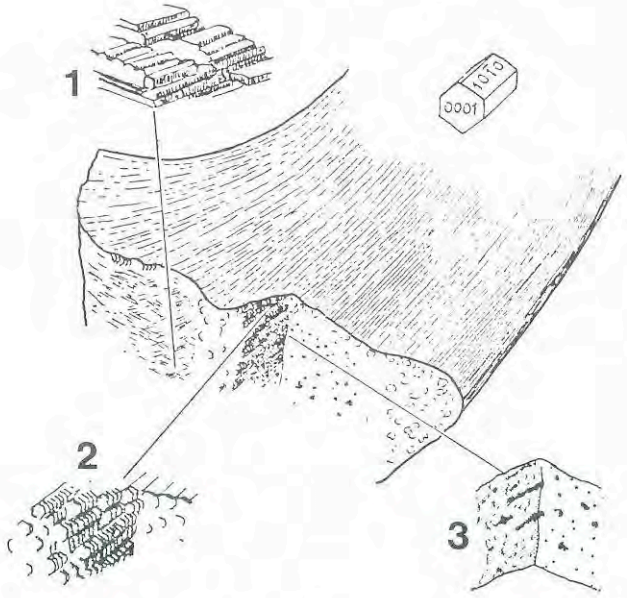

Fig. 2. Drawing illustrating orientation of crystallites within individual lamella of a conodont element, magnification is approximately 700x. 1--elongate crystallites of hyaline matter; 2--alignment of surface crystallites; 3--internal apatitic white matter contains some cavities and bubble structures. From Lindström and Ziegler (1981) by permission of University of Kansas and the Geological Society of America.

TABLE 1. Lattice parameters of apatites.

	a (Å)	c (Å)
Biogenic		
human enamel[1]	9.441 ± 0.003	6.882 ± 0.003
human dentine[1]	9.419 ± 0.003	6.880 ± 0.003
human bone[1]	9.417 ± 0.003	
shark enamaloid[1]	9.382 ± 0.003	6.880 ± 0.003
conodont elements[2]	9.37	6.91
conod. w/bas.mat.[2]	9.35	6.90
Igneous/Sedimentary		
Durango, MX (F-Ap)[1]	9.375 ± 0.003	6.880 ± 0.003
Hly.Spr. GA (OH-Ap)[3]	9.422 ± 0.003	6.880 ± 0.003
Libby, MT (SrF-Ap)[4]	9.41	6.91
marine phosphorite[1]	9.322 ± 0.003	6.882 ± 0.003

[1]LeGeros, 1981
[2]Pietzner *et al.*, 1968
[3]Mitchell *et al.*, 1943
[4]Deer *et al.*, 1962

Most euconodont elements are apparently composed of two types of apatite. The albid cusps and denticles of the crown contain a core of white matter and are high-phosphate apatite. The outer hyaline portion of the crown of a conodont element is composed of high-carbonate apatite (Wright *et al.*, 1988; Wright and Conca, 1988). This is inferred from two lines of evidence. Carbonate content of bulk conodonts determined by infrared spectroscopy is about 2 wt.% (Pietzner *et al.*, 1968; James Conca, 1988, personal communication); and sodium contents are inversely proportional to calcium and phosphate contents. Plate 2 shows a scanning electron photomicrograph of a polygnathiform conodont platform (Pa) element that has been analyzed for several major and trace elements using the JEOL 8600 Superprobe. Figures 3a, b, and d are analyses of 10-μm electron beam widths across the hyaline margins of the platform and lower and upper denticle areas, respectively. Figure 3c shows analyses of 10-μm electron beam widths down the axis of the denticles, moving from the albid core, which contains white matter of one cusp, to the albid core, which contains white matter of the next cusp. The last analysis in this sequence is once again on the hyaline margin. There is a consistent coupling of high sodium contents with low calcium and phosphate contents and vice versa in all of these analyses. Furthermore, elemental totals are low and electron beam damage is greater in analyses where sodium contents are larger, suggesting volatilization of lighter elements such as carbon and oxygen of the carbonate ion. These data support the observations of Pietzner *et al.* (1968) that white matter is low in carbonate and organic matter in comparison to the hyaline portions of conodont elements.

The discovery of the two types of apatite comprising the crowns of conodont elements is evidence that a different organic template is required for deposition of each type of apatite within the tissue matrix. Because of the greater stability of high phosphate apatite in aqueous solution the compositional difference provides further constraints on the function of conodont elements and information on which of the conodont surfaces were more resistant to exposure. The zone of contact between the two types of apatite may be an area of structural weakness. This contact zone approximates the area along which breakage and subsequent loss of Ordovician and younger conodont denticles and cusps commonly occurs.

LeGeros (1981) reported that the incorporation of sodium into apatite precipitated from aqueous systems is facilitated by the coupled substitution of sodium and carbonate for calcium and phosphate. Additionally, sodium and carbonate contents are greater in human bone and dentine than they are in tooth enamel. In this regard, human tooth enamel is similar in composition to the albid cusps and denticles of conodont crowns, whereas dentine is similar to the hyaline portions of the crowns. However, their locations in conodont elements are reversed or inside out.

Many cations substitute for Ca^{2+}. In general, cations with ionic radii larger than calcium produce expansion of both axes, and conversely, substitution of cations with smaller ionic radii than calcium produces contraction of one or both axes (LeGeros, 1981). Calcium occupies two lattice sites in apatite. Four calcium atoms occupy Ca (I) positions and are in nine-fold coordination with oxygens from six different phosphate tetrahedra. Six calcium atoms are in Ca (II) positions in irregular seven-fold coordination with one hydroxyl ion and six oxygens from five different phosphate tetrahedra (Eanes, 1973).

These considerations can be important in understanding why one substituent is favored over another. For example, recent studies (Wright, 1985; Wright *et al.*, 1987a) have shown that the postmortal substitution of total rare earth elements (REE) in conodont apatite is about one weight percent and that fractionations of one or more of the REE provide information useful for environmental interpretation as discussed below. Of the REE group, neodymium and samarium consistently show the highest concentration levels in fossil apatite. Table 2 gives the ionic radii of calcium in comparison to eight of the REE at six-, seven-, eight-, and nine-fold coordination. The ionic radii of neodymium and samarium in seven-, and nine-fold coordination are closest in size to the ionic radius of calcium in these coordination states. This indicates that the substitutiton of rare earth elements for calcium in apatite is controlled by ionic radius producing an abundance peak at Nd-Sm, which gives the characteristic concave-downward shape to REE patterns of conodont apatite.

In a comprehensive review article by LeGeros (1981) a number of general observations were made regarding the effects of the substitution of various ionic species for calcium, phosphate or hydroxl on the crystal structure of biogenic apatites. Cations with ionic radii larger than Ca^{2+}, e.g., Sr^{2+}, Pb^{2+}, Ba^{2+}, lanthanides, and actinides, preferentially substitute in apatite over cations with ionic radii smaller than Ca^{2+}. Substitution of fluoride increases crystallinity; substitution of strontium, sodium, and lithium has no effect on crystallinity; whereas substitution of carbonate, barium, lead, magnesium, cadmium, manganese, zinc, and aluminum decreases crystallinity. The presence of some ions in aqueous solution act as poisons to inhibit the formation of apatite and can even induce the precipitation of a precursor apatite phase or an amorphous phase. These ions include reduced iron and chromium, plus cobalt, nickel, and magnesium. However,

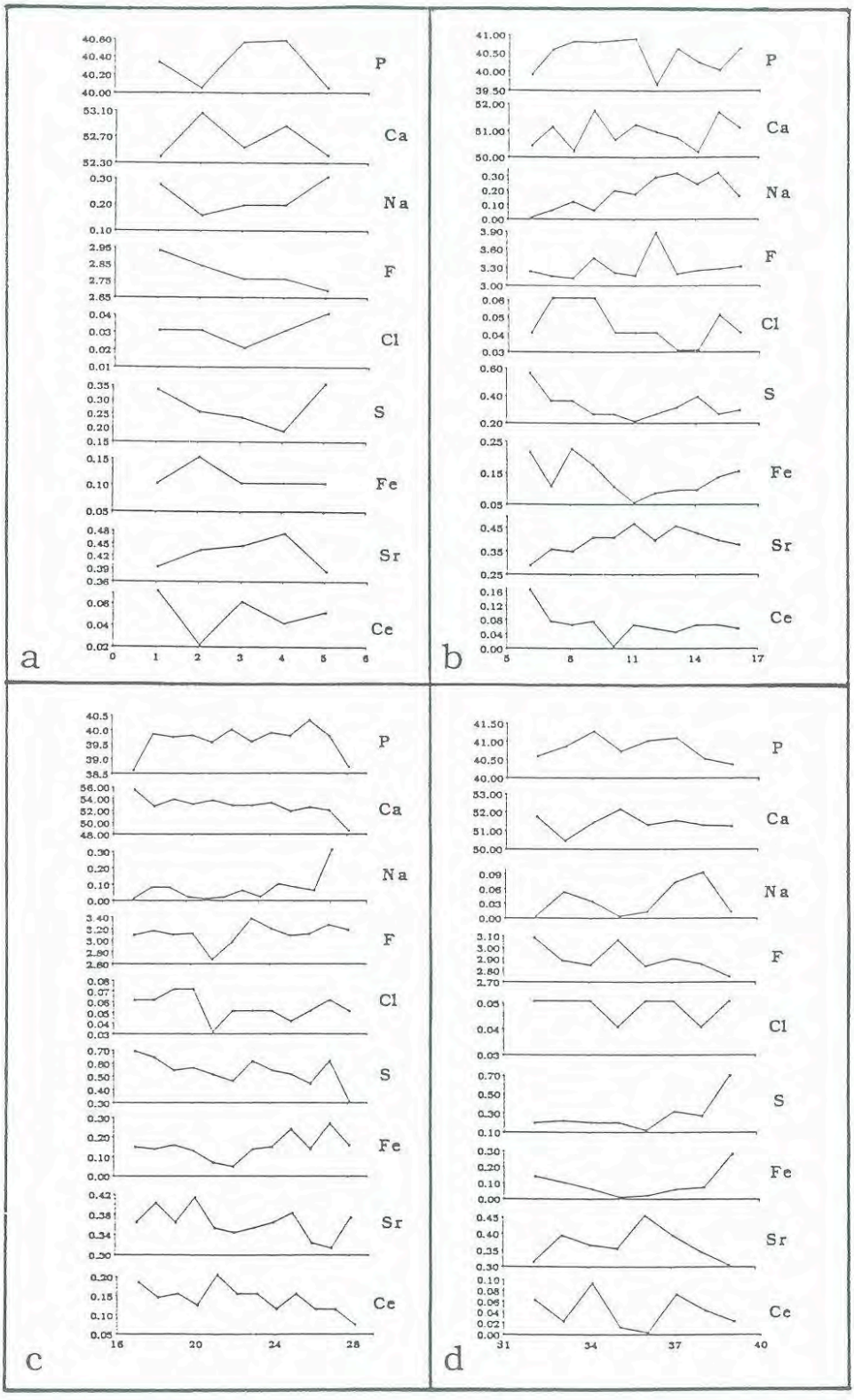

Fig. 3. Microchemical analyses of a polygnathiform conodont; a. chemical analyses 1 through 5 across the platform margin; b. chemical analyses 6 through 16 along the lower denticle margin; c. chemical analyses 17 through 28 through the core of the denticle region; d. chemical analyses 32 through 38 along the upper denticle margin.

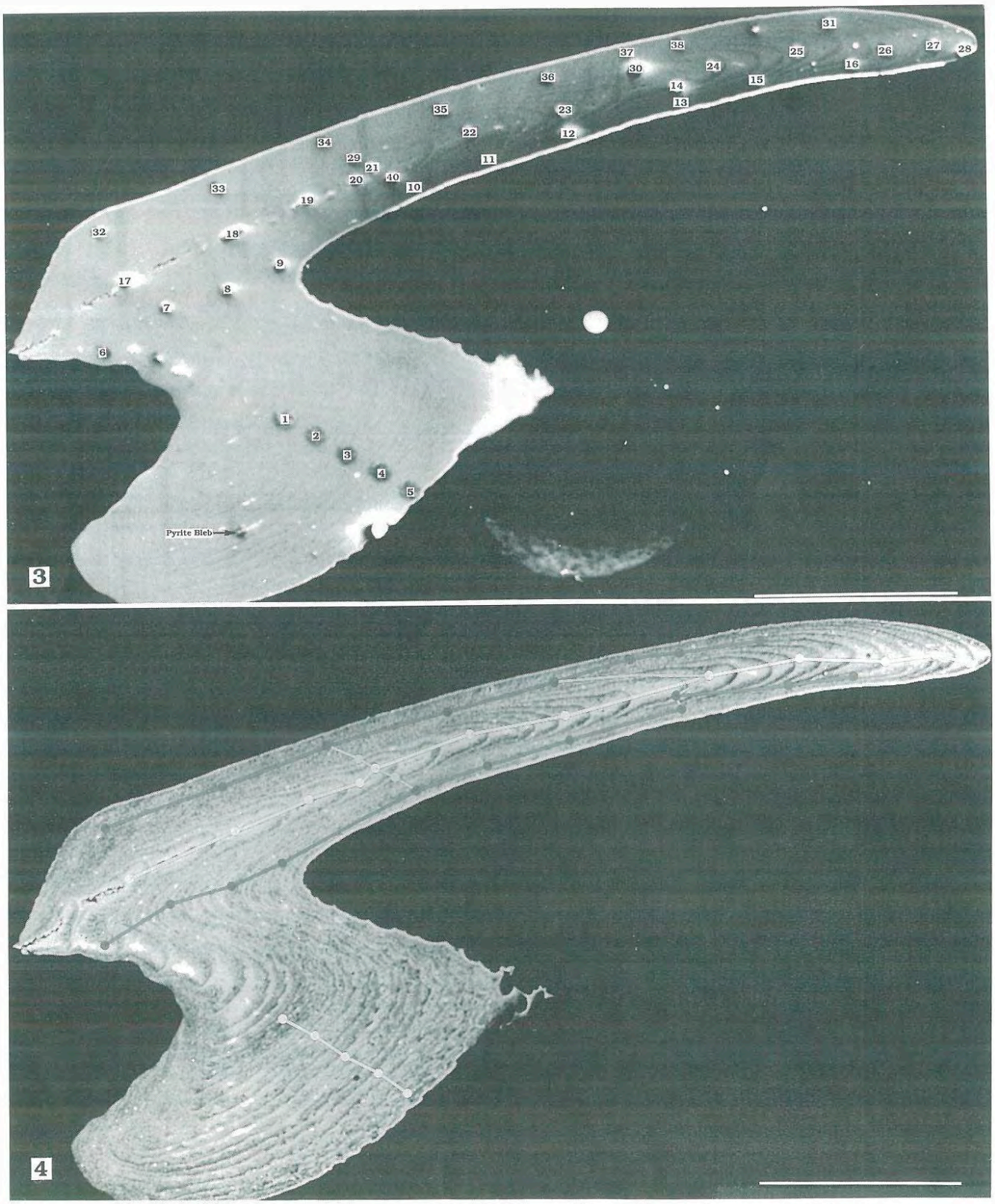

Plate 2. Scanning electron photomicrograph of a polygnathiform Pa or platform conodont element. Fig. 3. Chemical analysis points are labeled. Fig. 4. Lines indicate analysis transects shown as line plots of groups of elements in text Figure 3. Scale is 100 μm.

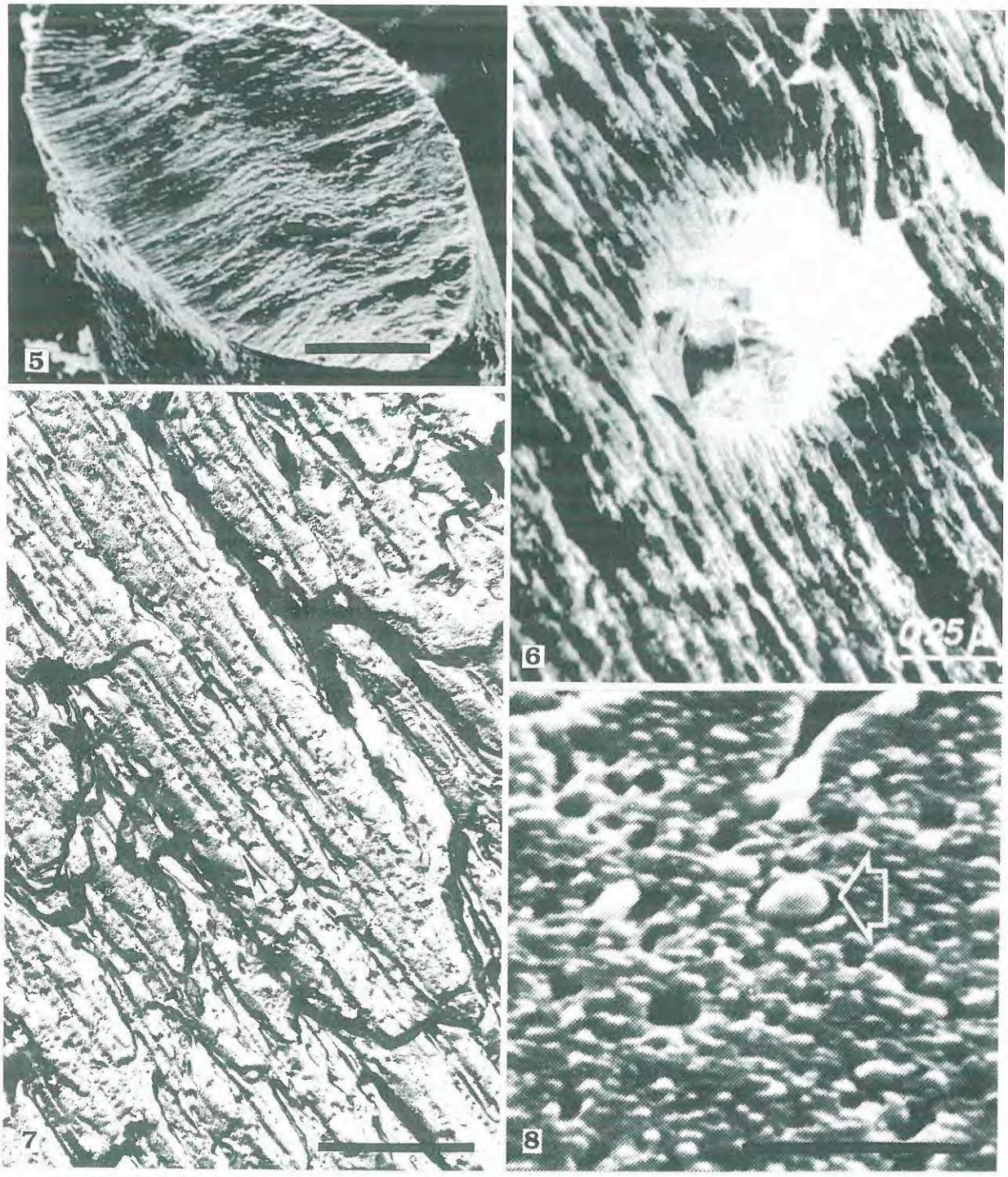

Plate 3. High resolution electron photomicrographs of microspheres in white matter of conodonts. Fig. 5. Broken surface of main denticle of a *Cordylodus* shows approximately parallel striations, scale is 50 μm (Pietzner *et al.*, 1968, Plate 27, Fig.1). Fig. 6. Microtome section of *Hindeodella* shows alternation of thick and thin parallel layers of coarse and fine apatite crystallites in white matter, and apatite crystals radiating from an empty cavity, scale is 0.25 μm (Pietzner *et al.*, 1968, Plate 21, Fig. 3). Fig. 7. Longtitudinal section through *Polycaudus bidentatus* shows the long parallel rods of apatite crystals arranged in microlayers within lamellae, microspheres are aligned in

oxidized iron and chromium in the aqueous growth medium have no effect on crystallinity or crystallization of hydroxyapatite.

Temperature and pH also influence the crystal growth and the extent of incorporation of some substituents. Higher temperatures favor increased crystallinity as well as crystallite size. At lower pH, the incorporation of fluorine is enhanced, but strontium substitution increases with increasing pH. However, simultaneous substitution of fluorine and strontium increases the resistance of apatite to acid dissolution. Additionally, strontium substitution reduces the extent of carbonate incorporation, and therefore increases apatite stability. Carbonate for phosphate substitution is favored in aqueous systems, whereas carbonate for hydroxyl substitution is favored in non-aqueous systems. Biological apatites, like apatites from aqueous systems, discriminate against the incorporation of chloride, and favor the substitution of fluoride for hydroxyl. Fluorine substitution reduces, and carbonate substitution increases, the solubility of biogenic apatite.

The above relationships have been determined in the course of bone and dental research but may have implications for secular variations in the chemistry of the hydrosphere and atmosphere throughout the Phanerozoic. These variations are recorded in conodonts and other forms of fossil apatite as shifts in concentrations of trace elements or ionic species. Examples are: 1) elevated strontium concentrations in Cambrian conodont apatite, which gradually decrease throughout the Paleozoic (Kovach, 1981); 2) variations in the enrichment (Cambrian to Devonian and Triassic) or depletion (Late Devonian to Late Permian) of cerium in conodont apatite (Wright 1982; 1985; Wright *et al.*, 1987a); and 3) the change from monomineralic (carbonate-substituted) to bimineralic (normal phosphate plus carbonate-substituted) conodont apatite near the Cambrian-Ordovician boundary.

Pertinent Structural Details of Conodont Elements

Early visual observations of whole and thin-sectioned conodont elements using light microscopy provided an extremely accurate depiction of the internal structure and morphologic constituents of different types of conodont elements. Sophisticated high-resolution electron beam imaging has confirmed the conclusions of the early studies and enhanced knowledge of many details of conodont ultrastructure while at the same time raising additional points of inquiry. The following review will outline the major structures of euconodonts or true conodonts which range from Late Cambrian to Triassic. Three evolutionary antecedents have been proposed for euconodonts: protoconodonts and paraconodonts (Bengtson, 1976), which originated near the Precambrian-Cambrian boundary; and *Fomitchella* (Dzik, 1986) with origins in the Early Cambrian. All three have elements composed of phosphatic lamellae. Their main differences are in the amount of preserved organic matter and the probable mode of lamellar accretion. However, the origin of euconodonts is still unresolved.

Crown and Basal Filling

Conodont elements are composed of two basic components, the crown and the basal body or filling. Both the crown and the basal filling consist of apatite lamellae that were accreted concentrically. The lamellae of the crown are continuous around the upper surface, whereas the lamellae of the basal filling are not always continuous around the lower surface (Aldridge, 1987). Apatite crystallites of the basal filling are smaller than those of the crown, and do not have the parallel orientation of crystallites within lamellae that is a feature of the crown. The basal material contains numerous holes or cavities as well as apatite microspheres (Pietzner *et al.*, 1968; Lindström and Ziegler, 1981). Figure 1 is a generalized sketch of a simple platform conodont element showing orientations of the crown and the basal filling. The concentric growth lamellae curve around the growth axis of each denticle and show some continuity into the less distinct lamellae of the basal body (Lindström, 1973).

Lamellae

The crown is composed of parallel lamellae made up of microlamellae that consist of elongate parallel rods of apatite. Under normal growth rate conditions Lindström and Ziegler (1981) state that the crystallites are "arranged with prism surfaces parallel to the direction of growth." In other words, the c-axes of the crystallites are perpendicular to the direction of growth, or parallel to the outer surface of the element. This crystal growth orientation influences the surface ornamentation producing fine striae (Figure 2) and 120° angles at the juncture of longtitudinal facets (Lindström and Ziegler, 1981). The lamellae vary in thickness, probably as a function of growth rate, and are separated by interlamellar spaces, which contain original or remnant organic matter. The interlamellar spaces were one pathway for the incorporation of chemical species from the environment of deposition, and are commonly the site of pyrite deposits (note bright blebs of pyrite on Plate 2, Fig. 3, adjacent to analyses points 1 through 5).

White Matter

White matter is present in denticles and along the growth axis in the crown. It has been referred to as cellules, cancellated structure, or postmortal vesicles (Lindström and Ziegler, 1981) and is more finely crystalline than hyaline material. White matter contains irregular to subspherical holes or cavities, usually < 1.0 μm in diameter, that do not seem to be interconnected (Pietzner *et al.*, 1968; Barnes *et al.*, 1973). Microspheres up to 1.0 μm in diameter have been observed in white matter as well as aligned in rows along individual apatite crystallites within lamellae (Plate 3, Figs. 7 and 8). Plate 3 illustrates the structure of white matter; approximately parallel striations separate alternating coarse and fine crystalline layers (Plate 3, Fig. 5) and apatite crystallites form a radiating halo or layer around an empty cavity (Plate 3, Fig. 6).

---

rows along the individual prismatic crystallites. Scale is 1 μm (Barnes *et al.*, 1970, Plate VII, Fig. 1). Fig. 8. Pebbled character of surface of white matter resulting from many microspheres, some occupying holes. Scale is 5 μm (Barnes *et al.*, 1973, Plate 8, Fig.13). By permission of Senckenberg Forschungsinstitut, Pietzner *et al.* (1968); by permission of Royal Ontario Museum, Barnes *et al.* (1970) and by permission of Geological Society of America, Barnes *et al.* (1973).

TABLE 2. Ionic radii of Ca and REE in apatite.*

	VI	VII	VIII	IX
Ca^{2+}	1.00	1.06	1.12	1.18
La^{3+}	1.032	1.10	1.160	1.216
Ce^{3+}	1.01	1.07	1.143	1.196
Ce^{4+}	0.87	-	0.97	-
Nd^{3+}	0.983	-	1.109	..163
Sm^{3+}	0.958	1.02	1.079	1.132
Eu^{2+}	1.17	1.20	1.25	1.30
Eu^{3+}	0.947	1.10	1.066	1.120
Tb^{3+}	0.923	0.98	1.040	1.095
Yb^{3+}	0.868	0.925	0.985	1.042
Lu^{3+}	0.861	-	0.977	1.032

*Shannon, 1976

Microspheres

Microspheres of calcium phosphate are found in most tissues, from bacteria and protozoans to multicelled organisms, ranging from inarticulate brachiopods to fish and humans. These microspherical structures are produced within the golgi apparatus in the osteocyte, expelled to extracellular space, and utilized both to build structural supports, e.g., teeth and bones, and for metabolic activity. In summarizing bone formation theory, Pautard (1981) stated: "The present evidence suggests that mature bone is not a continuous and homogeneous bed of mineral enclosing a framework of collagen fibers, but a population of microspheres in various arrangements and modifications which remain intact throughout the life of the tissue and which may be removed or repositioned as a result of metabolic demand. The mineral of bone is therefore initiated within the osteocyte, migrates to a specific location as part of a microsphere and matures in the extracellular space, undergoing chemical and physical changes according to its site and history." Figure 4 illustrates the origin and progress of a microsphere from osteocyte to bone. Microspheres in protozoan, whale and human cells occur as mineral clusters with radiating apatite crystallites and range in size from 0.1 to 3 μm.

Microspheres in conodont elements probably represent the normal process of biogenic apatite formation. In this scenario, cavities are the former positions of golgi apparatuses, and microspheres represent the extracellular mode of transfer of apatite building blocks to their final destination. If true, the same process of bone and tooth formation has been utilized for over 520 million years. Plate 4 shows two cordylodan conodont elements and details of each one to illustrate the continuity of lamellae from the hyaline, high-carbonate lower crown to the high-phosphate white matter in the denticles. Plate 4, Fig. 12, is a detail of a zone of resorption or fracture in the white matter with subsequent regeneration that produced an offset in lamellae of the white matter, but maintained lamellar width.

Conodont Geochemistry

Modern Analogues for Conodont Apatite

Trace elements, including naturally occurring stable isotopes and radiogenic isotopes, are incorporated into biogenic apatite postmortally and penecontemporaneously during the deposition and early burial of the individual particles of tooth and bone. Because fish debris is the modern analogue for conodont apatite (Wright, 1982; 1985; Shaw, 1984), knowledge of the mode and rate of trace element incorporation into extant fish debris from modern seawater is essential to the understanding and interpretation of trace element acquisition by fossil conodont apatite from ancient oceans. Figure 5 shows the difference in rare earth element (REE) contents between shark teeth *in vivo* (Wright *et al.*, 1984) and after

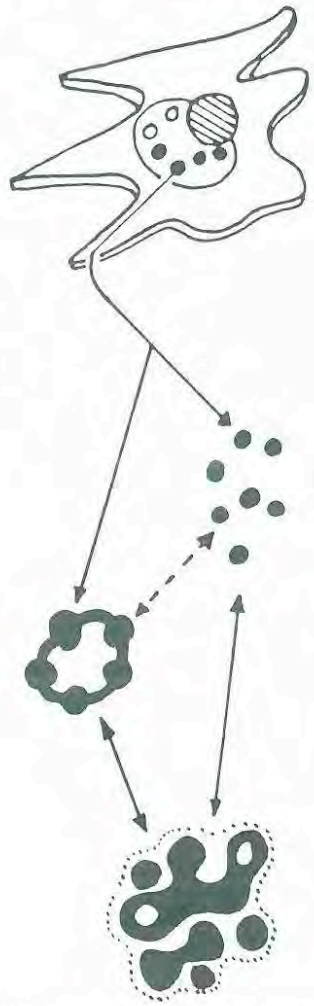

Fig.4. Schematic representation of microsphere formation from origin in the osteocyte to use in building human bone or for metabolism. From Pautard (1981) by permission of Pergamon Press.

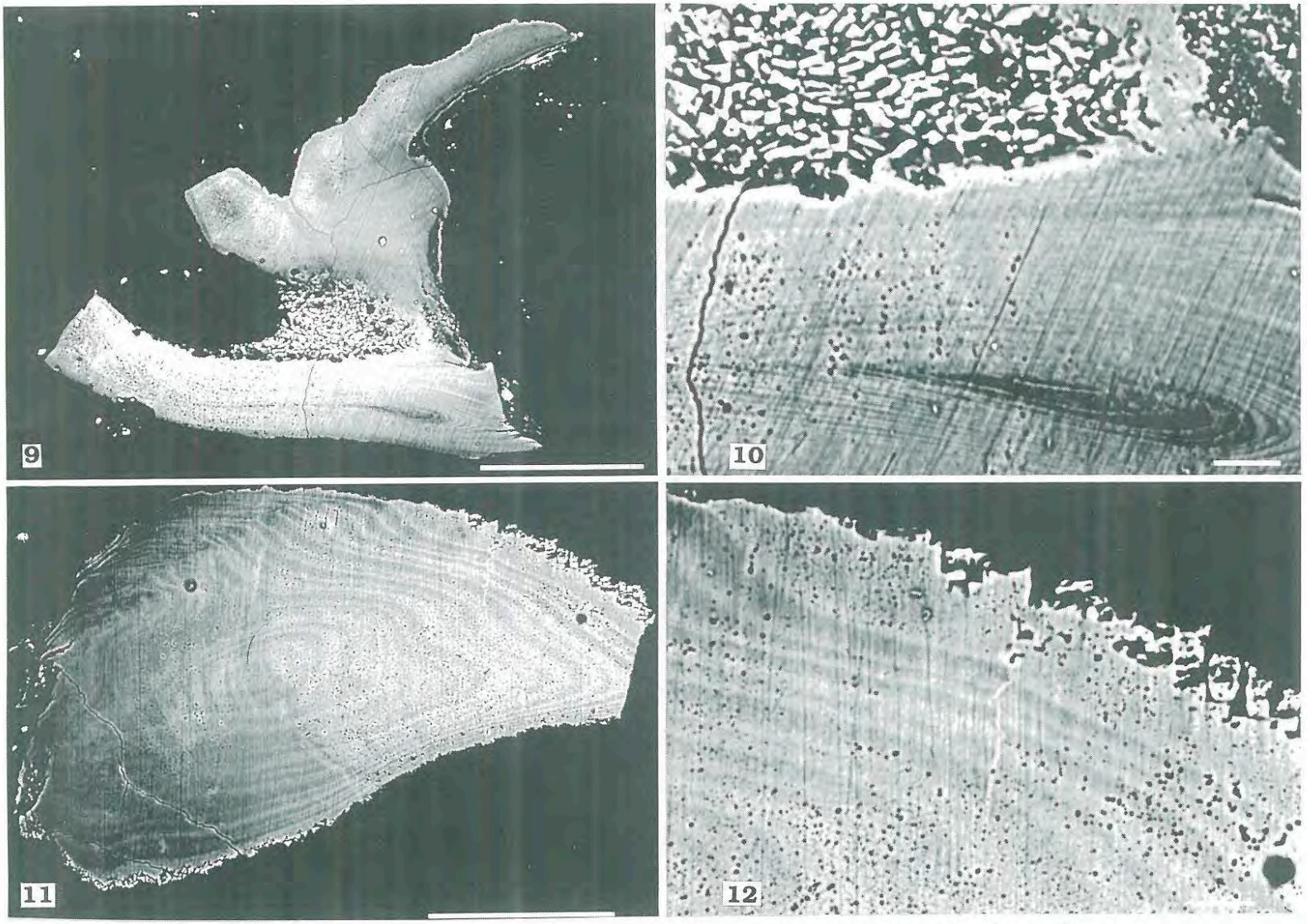

Plate 4. Figs. 9,10. *Cordylodus intermedius*. Figs. 10,11. *Cordylodus rotundatus*. Fig. 9. Shows main denticle, three cusps, and random orientation of apatite crystallites between main denticle and cusps. White matter with numerous cavities or holes is present in each denticle, scale is 100 μm. Fig. 10. Detail of Fig. 9, main denticle, showing continuity of lamellae from hyaline portion of crown into white matter, scale is 10 μm. Fig. 11. Main denticle showing boundary between white matter and hyaline lamellar portion. Lamellar structure is continuous throughout, scale is 100 μm. Fig. 12. Detail of Fig. 10, zone of resorption or fracture in white matter with regeneration producing an offset in the lamellae, but maintaining lamellar width, scale is 10 μm.

deposition in oxidized red clay sediments (Bernat, 1975). The fish apatite REE patterns are compared with Pacific (Goldberg *et al.*, 1963) and Atlantic (Elderfield and Greaves, 1982) seawater. The REE patterns of shark teeth are similar to the REE patterns of bones and teeth from salmon and other freshly caught fish (Wright, 1985) and show strong fractionation of the REE. These fractionations are the result of biological mediation during the process of tooth and bone formation. However, the REE patterns of fish debris after deposition acquire a different signature, and in Pacific fish debris the signature resembles the REE pattern of Pacific seawater (Figure 5). The Pacific fish debris REE patterns shown are from sediment cores taken in red clay sequences from horizons at 4 cm to 6 m below the sediment-water interface. Despite the differences in age represented by differences in sample position in the cores, the REE patterns are the same; they each represent highly-enriched, non-fractionated, fingerprints of Pacific seawater. The replication and retention of the seawater REE pattern in biogenic apatite implies that biogenic apatite incorporates trace elements after postmortal deposition in the sediments in the same proportions that the trace elements are present in the aqueous environment, but at greatly enriched concentration levels. Futhermore, the trace element signature of the depositional environment is retained through subsequent burial, compaction and diagenesis processes. Similar results have also been observed in fish debris samples from two cores taken on the Peru margin and the Gulf of California (Wright *et al.*, 1987a).

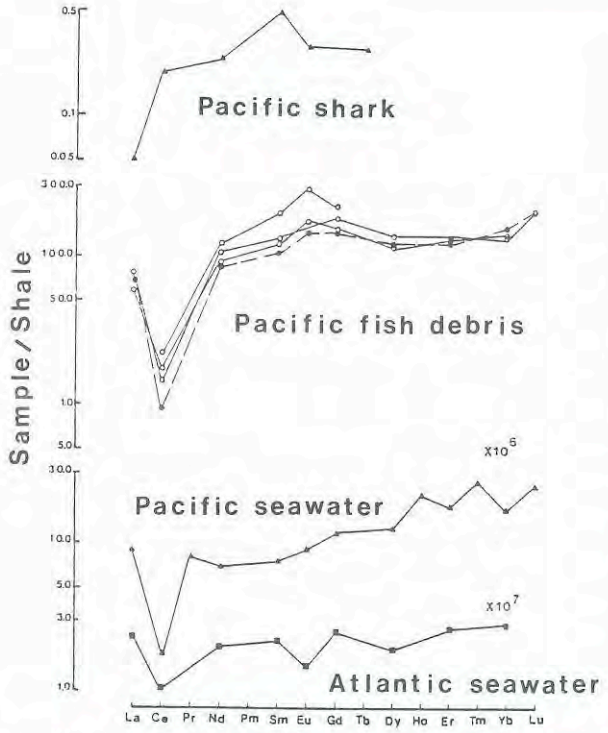

Fig. 5. Shale-normalized REE patterns of freshly-caught fish (Wright *et al.*, 1984), fish debris from the Pacific basin abyssal plain (Bernat, 1975), Pacific seawater (Goldberg *et al.*, 1963) and Atlantic seawater (Elderfield and Greaves, 1982). REE are normalized to shales to remove the odd-even effect of elemental abundances. Note that the Pacific and Atlantic seawater REE patterns are six and seven orders of magnitude higher, respectively, than their actual normalized concentrations in seawater, for easier comparison of the three log-scale plots of REE abundances. From Wright *et al.* (1984) by permission of the Geological Society of America.

This observation is borne out by further studies of REE and other trace elements in fish debris from oxidizing, sub-oxic, and reducing clay sequences at numerous locations in the Pacific, Atlantic, and Mediterranean basins (Elderfield and Pagett, 1986; Wright, 1985; Wright *et al.*, 1987a). Figure 6 shows two of the factors that influence the incorporation of REE into biogenic apatite: rate of sediment accumulation and redox conditions of the water masses overlying the depositional environment or dominating a seawater basin. Because Nd has the highest concentration levels of the REE in biogenic apatite, it is used as a proxy for the total acquisition of REE. Figure 6 illustrates that Nd concentrations are inversely proportional to the sediment accumulation rate. Abyssal plain pelagic sediments reflect the slowest rate of sediment accumulation, approximately 0.001 mm/yr, and therefore the longest exposure time of fish debris to interactions at the sediment-water interface, and concomitantly, the highest concentrations of Nd, up to several thousand parts per million (ppm) in a sample. Neodymium concentrations decrease when the rate of sediment accumulation increases, as seen in samples from the Peru margin and Guaymas Basin. In these samples sedimentation rates range from 0.021 to 0.14 cm/yr and from 0.12 to 0.38 cm/yr, respectively, and Nd concentrations are tens to hundreds of ppm and less than one to ten ppm, respectively. The processes that control the postmortal incorporation of REE into biogenic apatite obviously depend on length of exposure to interactions with seawater.

The second factor, redox conditions of the water masses, is represented by Ce_{anom}, which is a simple mathematical calculation of the enrichment or depletion of cerium relative to neighboring REE, La and Nd.

$$Ce_{anom} = Log\ [3Ce_n / (2La_n + Nd_n)]$$

where "n" is the shale-normalized concentration of the element. When Ce_{anom} has a value > - 0.10, cerium is enriched in the biogenic apatite sample, and when the Ce_{anom} value is < - 0.10, cerium is depleted in the sample. The enrichment or depletion of cerium in an environment results from fractionation and depletion of Ce by co-precipitation with metallic oxides under oxidizing conditions, or enrichment of Ce under reducing conditions when no mechanism is present to remove Ce from solution. Wright (1982;1985) and Wright *et al.* (1987a) provided details of the model of the redox control of Ce variations. Thus, fish debris from different environments carry signatures of the redox conditions dominant in the main water mass. The range of Ce_{anom} values in different seawaters is shown in the scale on the right side of Figure 6. The bar representing a profile of Black Sea water shows that even in surface, oxidizing waters of the Black Sea, Ce_{anom} values are positive. This indicates that in a seawater basin where deeper waters are anoxic, the cumulative buildup of cerium concentrations at depth is transferred across a concentration gradient to surface waters and reflected in an overall signature of anoxia throughout the basin (Wright et al., 1987a). The fish debris samples from many locations are plotted on the figure as a function of Ce_{anom} and Nd

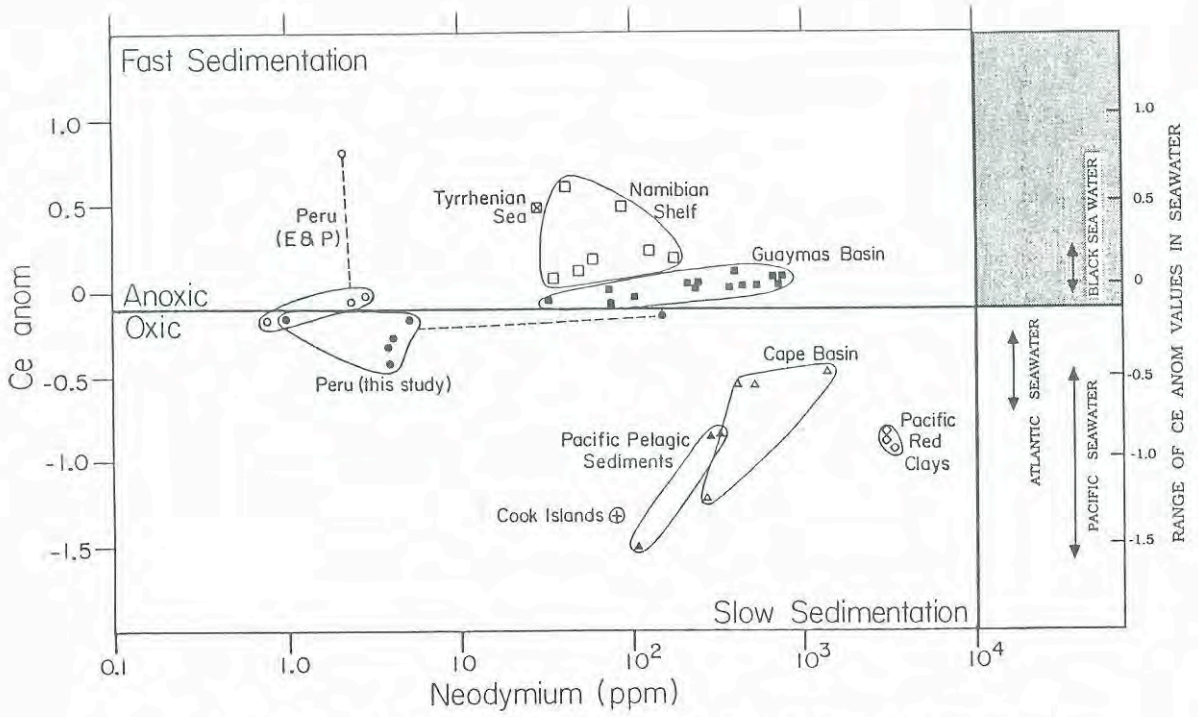

Fig. 6. Ce_{anom} versus Nd concentrations for fish debris from different depositional settings: Pacific red clays (Bernat, 1975); Cape Basin, Pacific pelagic sediments, Cook Islands, Namibian Shelf, Tyrrhenian Sea, and Peru shelf (Elderfield and Pagett, 1986); Guaymas Basin and Peru margin (Wright *et al.*, 1987). Scale on right shows range of Ce_{anom} values in seawater under differing redox conditions (Pacific seawater values from De Baar *et al.*, 1985; Atlantic seawater values from Elderfield and Greaves, 1982; and Black Sea water values from Kolesov *et al.*, 1975). This figure was modified and composited from figures by Elderfield and Pagett (1986) and Wright *et al.*(1987).

concentrations. Fish debris from deep water oxidizing sediments in the Pacific and Atlantic have very negative Ce_{anom} values indicating that Ce is removed by co-precipitation with metallic oxides. On the other hand, fish debris from cores on the Peru margin, Guaymas Basin, Namibian shelf and Tyrrhenian Sea, reflect the presence of elevated concentrations of Ce in Ce_{anom} values that are close to zero or positive. This is a result of the presence of suboxic to anoxic conditions in the overlying water masses where there is no mechanism to remove Ce from solution and therefore Ce is available for incorporation into the biogenic apatite of fish debris. These two factors are crucial in the environmental interpretation of the REE contents of conodonts as discussed later, but first additional evidence is provided to show that apatite retains the trace element signature of the paleoenvironment.

Absolute Age Dating Using Conodonts

Multiple splits of two Pennsylvanian conodont samples were analyzed for age determinations by the U-Th-Pb method of radiometric dating. Four splits of a conodont sample from the Ames Limestone from the Virgillian of eastern Ohio yielded ages that were in general agreement with the stratigraphic age. Four splits of a conodont sample from the lower Missourian Brush Creek Limestone from northern West Virginia gave ages that were not as accurate but still within two sigma error of the stratigraphic age (Kovach and Zartman, 1981). Fission track dating of conodonts from the Lower Mississippian Chappel Limestone from Texas also gave a reliable age (Sachs *et al.*, 1980). Two problems encountered in radiometric age determinations using conodont elements are the requirement of a large sample size (>15 mg) and unexplained discordant dates for multiple splits of the same sample. However, non-radiogenic Nd dating techniques (Shaw, 1984; Shaw and Wasserburg, 1985; Keto, 1987) of conodonts and inarticulate brachiopod shells from several Paleozoic horizons give absolute ages for the host carbonate rocks that are in agreement with the relative stratigraphic age, and show less discordancy among multiple sample splits. Additionally, reliable Nd ages can be obtained from a very small amount of conodont sample material (< 1 mg) because of the consistently high concentration levels of Nd in biogenic apatite. Although preliminary, these age-dating studies provide additional confirmation that trace elements and their stable and radiogenic isotopes are incorporated syndepositionally into conodont apatite and retain a compositional signature that reflects the paleochemical marine environment. Detailed age-dating studies that are constrained by samples of conodont elements 1) from continental margin or open ocean depositional sequences, 2) with low CAI values to assure low temperature thermal history, 3) with trace element studies of the same sample splits, and 4) with multiple sample splits at adjacent

stratigraphic horizons, will provide the scientific rigor needed to supply numerical ages for biogenic apatite-bearing sediments throughout the Phanerozoic.

Organic Matter

The small quantity of organic matter associated with conodont apatite provides the dominant color centers for conodonts. Ellison (1944) and Lindström (1964) observed the color variations in conodonts; however, they were not studied rigorously until the work of Epstein *et al.* (1977) and Rejebian *et al.* (1987). Field data from the Appalachian Basin combined with experimental heating studies showed that the color changes are time and temperature dependent. Color changes occur systematically and are a function of thermal alteration of the small amounts of organic matter contained within the conodont apatite. The progressive and irreversible color changes have been assigned to a numerical color alteration index (CAI) on a scale of 1 to 8 (Epstein *et al.*, 1977; Rejebian *et al.*, 1987). Calibrated color changes of conodonts from pale yellow (CAI 1) through light to dark brown (CAI 1 1/2 to 4 1/2) to black (CAI 5) and from black to gray to white to clear (CAI 5 to 8) permit an assessment of the burial temperature of the conodont-bearing host rock up to 600°C. The lower CAI values (1 to 5) have been correlated with other indices of organic metamorphism and thermal maturity up to 400° C (Epstein *et al.*, 1977; Nowlan and Barnes, 1987). CAI values of conodonts are useful in a wide variety of practical applications including: hydrocarbon and mineral exploration; compilation of regional maps showing thermal trends and anomalies which are important for structural and tectonic interpretation (Harris, 1979; Legall *et al.*, 1982; Sandberg and Gutschick, 1984; Armstrong and Strens, 1987; Nowlan and Barnes, 1987); for the recognition of hotspot tracks (Legall *et al.*, 1982; Nowlan and Barnes, 1987); and to determine when the thermal history of carbonate rocks is suitable for paleomagnetic studies (Ripperdan *et al.*, 1987). These studies show that the organic component of conodont elements carries an index to the thermal history of the fossil material during postdepositional processes.

Recent analysis of the composition of the organic component of conodont apatite indicates that a wide variety of amino acids is present. Preliminary studies suggest that these primary organic constituents may show distinct groupings of amino acids reflecting taxonomic differences (Savage *et al.*, 1988).

Stable Isotopes

$^{87}Sr/^{86}Sr$, $^{143}Nd/^{144}Nd$, and $\partial^{18}O/^{16}O$ are stable isotopic pairs, which have been characterized in conodont and other biogenic apatites. The isotope systematics for Nd and for O in biogenic apatites were developed by Shaw (1985), Staudigel *et al.* (1985), and Kolodny *et al.* (1983), respectively. Strontium isotope systematics in biogenic apatites have not been clearly defined. To understand the significance of variations of each of these isotopic systems in conodonts, it is necessary to understand their systematics in modern seawater.

Values for Nd isotopes range widely in modern seawater; however, the water in each water layer in an ocean basin has a limited and characteristic Nd isotopic composition. The variability within an ocean basin results from the presence of chemically and physically distinct water masses distributed in horizontal layers in each ocean basin (Piepgras *et al.*, 1979; Piepgras and Wasserburg, 1980; 1982). The extreme variability of Nd isotopes in seawater is a result of the short residence time of Nd (and other REE) in seawater relative to oceanic mixing times, such that the isotopic signature of individual water masses tends to be conserved over the life of the entire water mass (Piepgras and Jacobson, 1988; Elderfield and Greaves, 1982). Thus, Nd isotopes can be used as tracers of modern oceanic circulation patterns (Piepgras *et al.*, 1979; Piepgras and Wasserburg, 1980; 1982). Staudigel *et al.* (1985) developed the systematic basis for the study of Nd isotopes in fish debris from Neogene sediments, showing that they retain the Nd isotopic signature specific to an ocean basin. The same reasoning can also be applied to the study of ancient ocean basins and circulation patterns by analyzing a marine phase that retains the Nd isotopic signature of the depositional environment. A few samples of conodont apatite, inarticulate brachiopod shells, and fish debris have been used to begin studies of Paleozoic ocean basin configurations and the connections of surface water masses (Shaw and Wasserburg, 1985; Keto and Jacobsen, 1987). Nd isotopic data of some conodonts but mainly of inarticulate brachiopods have been used to constrain paleogeographic reconstructions of the early Paleozoic, and indicate the presence of a physical barrier to circulation, e.g., a chain of islands, which separated northern and southern portions of the Iapetus seas or oceans (Keto *et al.*, 1987).

The strontium isotopic composition of modern seawater is a very different case in comparison to that of Nd. Strontium isotopes have a uniform value in the oceans (Faure *et al.*, 1965; Murthy and Beiser, 1968; Piepgras and Wasserburg, 1980) as a result of the long residence time of 10^6 years of Sr in seawater (Turner and Whitfield, 1979). Because of the long residence time of Sr, marine samples from different ocean basins will carry the same Sr isotopic signature at a given time interval. Construction of a curve that shows the temporal or secular variations in the Sr isotopic composition of seawater can provide information on the long-term geologic mechanisms that produce variability in Sr. The primary mechanisms that cause shifts in the Sr isotopic composition of seawater are weathering processes; orogeny resulting in emergent land masses; volcanic activity; rate of sea-floor spreading; extent of epeiric seas; and climatic processes, mainly rate and amount of global precipitation. Secular variations of Sr isotopes in calcite shell material and limestones were determined in corroborating studies by Peterman *et al.* (1970), and Veizer and Compston (1974). Further studies of carbonates and sulfates provided additional detail for the Sr isotope age curve (Brass, 1976; Clauer, 1976; Faure *et al.*, 1978). Figure 7 is a plot of the strontium isotope age curve. Greater detail was added to the curve by further studies using conodonts (Kovach, 1980; Burke *et al.*, 1982), fish and shark teeth, calcite fossils, limestones, dolomites, and evaporites (Burke *et al.*, 1982; Koepnick *et al.*, 1985). Keto (1987) modeled Sr isotopic variations for the past 750 my (part of her analytical studies are of conodonts) and determined that the main source of Sr variation results from riverine input rather than hydrothermal activity. The most important factors defining shifts in the Sr isotope age curve are 1) paleoclimatic changes in temperature and global precipitation, which resulted in increased weathering of continental crust, and 2) orogeny, which produced emergent land masses.

The primary fractionation mechanism of oxygen istopes re-

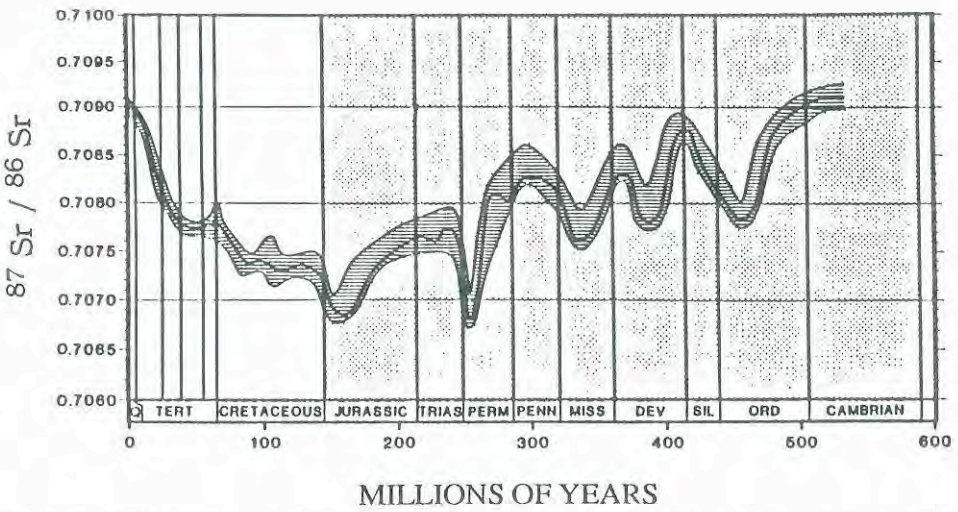

Fig. 7. $^{87}Sr/^{86}Sr$ age curve for the Phanerozoic, for any given time the correct seawater value probably lies within the shaded band. The line drawn through the band is an estimate of the seawater ratio vs. time. A portion of the curve from the Paleozoic was derived from analyses of conodonts. From Koepnick *et al.* (1985) by permission of Elsevier Science.

sults from the evaporation/precipitation cycle. Evaporation preferentially removes slightly more light oxygen relative to heavy oxygen. Precipitation in the form of rain or ice, deposits slightly more heavy oxygen first, closer to the source of the moisture, so that the isotopic signature becomes lighter moving away from the source region where evaporation moved the water to the clouds. $\partial^{18}O$ values are related to salinty in that the oxygen isotopic signature of seawater is dependent on the amount of oxygen stored on continents in the form of glacial ice which is enriched in ^{16}O relative to seawater. Oxygen isotope studies of forams and other calcitic fossils whose carbonate shells are grown in equilibrium with seawater oxygen, and of Antarctic ice cores have provided a temperature curve for the Cenozoic and part of the Mesozoic (Emiliani, 1955; Shackleton and Kennett, 1975; Savin, 1977). Several studies opened the possibility of determining paleotemperatures of Paleozoic oceans by developing the systematics for analysis of phosphates (Longinelli and Nuti, 1973a; Shemesh *et al.*, 1983a) and providing evidence that biogenic apatite is precipitated in the organism in isotopic equilibrium with the water of the growth environment (Kolodny *et al.*, 1983). Studies of $\partial^{18}O$ of conodonts (Luz *et al.*, 1983; Geitgey and Carr, 1987; Karhu and Epstein, 1986) and phosphate-chert pairs (Karhu and Epstein, 1986) at several stratigraphic levels in the Paleozoic have given results that do not clearly relate to absolute ocean temperatures. The ambiguity of these studies results from one of several factors: no knowledge of the oxygen isotopic composition of Paleozoic seawater, sampling bias towards shallow carbonate seas, or lack of proper mineralogical and stratigraphic constraint on sample material. However, the results are useful for determining relative temperature variations and their effect on conodont diversity and distribution (Geitgey and Carr, 1987).

Trace Elements

In the first geochemical studies of conodonts, Pietzner *et al.* (1968) showed that a wide variety of trace elements were incorporated heterogeneously into conodont apatite. They found that the basal filling contained higher concentrations of many trace elements than were contained in the crown. Bradshaw, Noel and Larson (1973) detected the presence of an additional suite of trace elements in conodonts, bringing the total number of trace elements that are detectable in conodont apatite to 43. Kovach (1981) analyzed 68 samples of Ordovician through Triassic conodonts and found a general decrease in Sr content from 20,900 to 1560 ppm corresponding with decreasing age. Wright (1982; 1985) systematically determined quantitative concentrations of 34 trace elements in more than 200 conodont samples representing a worldwide sample distribution and the entire range of conodonts. Developmental studies on the analysis of conodonts by inductively coupled plasma-mass spectrometry indicate that additional elements will be determined in conodont apatite (M.R. Smith, personal communication). Wright and Conca (1988), in microchemical mapping studies of several conodont crowns, illustrated quantitatively that the trace and minor element distribution is heterogeneous. Figure 3 shows analyses of 38 ten-μm points on a single polygnathiform Pa element. Comparison of the line plots of the elements at each point shows that there is no systematic enrichment or depletion of any element moving from the margin to the interior of the conodont. This lack of change indicates that diagenesis has not affected the trace element contents of the conodont apatite by the addition, removal, or migration of trace elements from the interior to the exterior portions of the conodont. The following two major systematic studies of the trace element contents of conodonts have provided useful information for interpretation of paleochemical environments and for chemostratigraphic correlation.

Paleoredox Conditions of Ancient Oceans

Rare earth element (REE) contents of marine biogenic apatite of conodont elements and other phosphatic fossil material from Paleozoic and Mesozoic stratigraphic horizons with a

worldwide sample distribution show secular variations in Ce_{anom} (Figure 8). The variations result from changes in the oxidation-reduction regime that was prevalent in these ocean basins at the time of deposition. Fossil apatite samples are from normal, shallow-water carbonate sequences that were deposited under oxidizing conditions; however, the signature of anoxic conditions, which dominated other portions of the water column, was transferred to oxic surface waters and recorded in the REE patterns of biogenic apatite samples deposited there (Wright, 1985). These data support earlier models which predicted that oceanic anoxic conditions had been widespread in Cambrian through Devonian and again in Permian-Triassic seas (Degens and Stoffers, 1976; Berry and Wilde, 1978).

The secular variation of Ce_{anom} indicates that early Paleozoic oceans were dominated by anoxic conditions. There is a shift in the Devonian to generally oxidizing conditions, which persisted throughout late Paleozoic seas until Late Permian to Early Triassic times when the paleoredox environment may have returned to low oxygen to anoxic conditions. Oxidizing conditions became dominant again in Late Triassic and Jurassic seas. The bimodal distribution in phosphatic fossils from the Upper Jurassic of Solnhofen basin reflects shifts from normal oxidizing conditions (samples from clay layers) to catastrophic

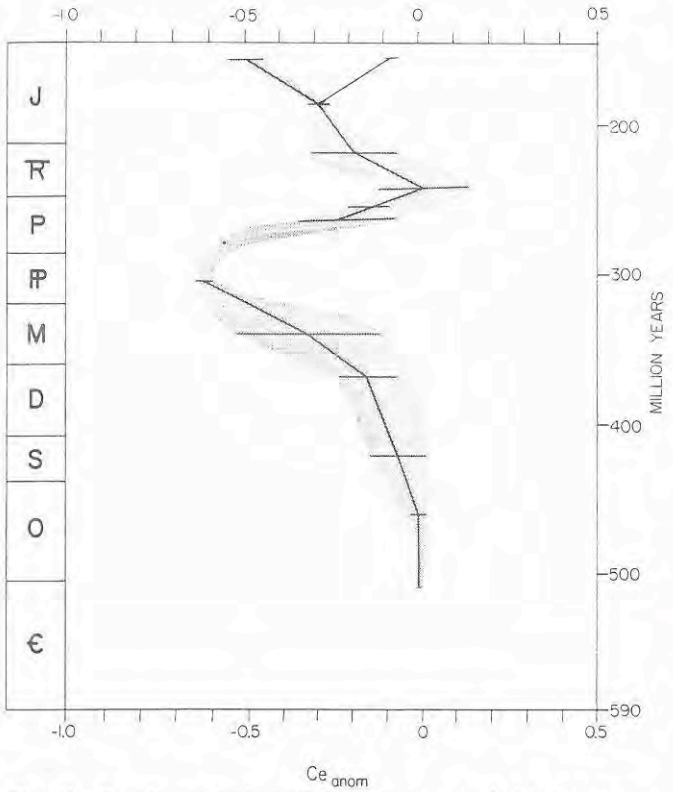

Fig. 8. Secular variation of Ce_{anom} as recorded in biogenic apatite of conodonts, and other phosphatic fossils. Values are calculated for groups of samples at a single time interval. The curve was drawn through the average value for the time interval showing a two sigma error bar as the shaded region associated with each value. Full details of analyses and locations are given in Wright (1985) Wright *et al.* (1987a).

deposition of thick coccolith layers during episodic red tides when anoxic conditions were dominant (De Buisonjé, 1972). More detailed studies of apatite faunas at stratigraphic horizons post-dating the extinction of conodonts in the Late Triassic will provide information on the redox conditions of younger oceans.

Studies of conodonts from Upper Devonian sections across the Frasnian-Famennian Stage boundary are being conducted as part of IGCP Project 216, Global Bioevents. These examine in detail some of the paleochemical changes that occurred in the Late Devonian when the world ocean shifted from the anoxic environment, which had dominated it for hundreds of millions of years, to perhaps the first recorded occurrence of generally oxidizing conditions similar to the modern ocean. Perhaps these trace element studies will provide additional information on the nature of the processes that produced mass extinction of some marine faunas.

Chemostratigraphy

Chemostratigraphic correlations of rock strata using the trace element signature of conodonts at a single biostratigraphic interval from widely separated geographic locations show evidence of synchronous paleochemical events in seawater. These chemical events are used to predict previously undetermined biostratigraphic horizons (Wright *et al.*, 1987b) as well as regional or global chemical events in earth history (Wright *et al.*, 1987a). Trace element studies of conodonts from Cambrian-Ordovician boundary sections in the western United States and southeast China were conducted to determine if correlatable chemical signatures were present. Two groups of trace elements showed correlation based on conodont biostratigraphy. The rare earth element group represented by Ce_{anom} of conodonts showed correlation among the western U.S. sections from Texas, Oklahoma, and Utah, but did not correlate to the Chinese section at Dayangcha. However, another group of trace metals, Sc, Cr, Co, Ni, Zn, Sb, Au, plus As, Th and Sr, had an excellent correlation among samples of conodont elements from all four sections. This group of metals was used to accurately predict the base of a previously undetermined conodont biostratigraphic horizon. The difference between the rare earths and the other group of trace elements is their residence time in seawater. The REE have a very short residence time in seawater, from tens to hundreds of years; therefore, fluctuations in Ce_{anom} provide a good regional correlation tool. The other group of trace elements has residence times from thousands to millions of years in duration and, therefore, are distributed more homogeneously within the world ocean to provide a method of global correlation. Other trace element correlation studies of whole rocks from the Ordovician (Wilde, 1987; Berry *et al.*, 1989) and from the Cretaceous-Tertiary boundary (Alvarez *et al.*, 1980) have also shown that trace elements are reliable correlation tools.

Conclusions

Conodont apatite allows exchange of the major cation, calcium, with trace constituents in seawater. However, after incorporation, the biogenic apatite system does not allow further exchange of trace elements with diagenetic waters. The mechanisms that govern these properties are not fully

understood; however, the trace elements supply an accurate signature of seawater and the depositional environment. The remnant paleochemical fingerprint has been shown to be extremely useful in many types of geologic interpretations, including secular variations of seawater chemistry; paleogeographic and paleoceanic reconstructions; chemostratigraphic correlations; relative temperature determinations; absolute age determinations of sediments; and deducing weathering rates, oceanic vs. continental crustal evolution, and connections between paleoceanic water masses. Detailed studies of the microchemistry and microstructure of conodont apatite have indicated that information on the evolution of apatite biomineralization processes is probably also retained in conodonts.

Acknowledgements. This manuscript benefitted considerably from careful and well thought out reviews by Dick Aldridge, Dave Clark, Jim Conca, Dave Hilliard, Gil Klapper, Don Piepgras, Charlie Sandberg, and Jeremy Stone. Very special thanks to Joseph Carter for his editorial expertise and encouragement. The work was generously supported by Battelle management, particularly John Latkovich, Bruce Kaiser, and Gene Eschbach. Microprobe studies were completed during independent postdoctoral research in residence at the Honors Department, Arizona State University, with the encouragement of advisor, Ted Humphrey, and with the assistance of Jim Clark and Jim Conca. Musical inspiration was provided by Mozart, Sting and Tracy Chapman.